Since January 2020 Elsevier has created a COVID-19 resource centre with free information in English and Mandarin on the novel coronavirus COVID-19. The COVID-19 resource centre is hosted on Elsevier Connect, the company's public news and information website.

Available online at www.sciencedirect.com
ScienceDirect
Journal of Inorganic Biochemistry 101 (2007) 89–94
Journal of Inorganic Biochemistry
www.elsevier.com/locate/jinorgbio

Studies on the interactions of Ti-containing polyoxometalates (POMs) with SARS-CoV $3CL^{pro}$ by molecular modeling

Donghua Hu [a,b], Chen Shao [a], Wei Guan [a], Zhongmin Su [a,*], Jiazhong Sun [c]

[a] Institute of Functional Material Chemistry, Faculty of Chemistry, Northeast Normal University, Changchun 130024, China
[b] Traditional Chinese Medicine Institute of Traditional Chinese Medicine Collage of Changchun, Changchun 130017, China
[c] State Key Laboratory of Theoretical and Computational Chemistry of Jilin University, Changchun 130000, China

Received 22 December 2005; received in revised form 14 August 2006; accepted 17 August 2006
Available online 5 September 2006

Abstract

Ti-containing α-Keggin polyoxometalates (POMs) have been proved with properties of both anti-tumor and anti-HIV (human immunodeficiency virus). The potential anti-SARS (severe acute respiratory syndrome) activity of the POMs $[\alpha\text{-}PTi_2W_{10}O_{40}]^{7-}$ isomers was investigated in this paper by molecular modeling method. The SARS 3c like protease, namely the SARS $3CL^{pro}$ is the key function protease for virus replication as well as transcription and thus can be taken as one of the key targets for anti-SARS drug design. Affinity/Insight II was used to explore possible binding locations for POMs/$3CL^{pro}$ interaction. Charges in the POMs were obtained from density-functional theory (DFT) method. The results show that POMs bind with $3CL^{pro}$ in the active site region with high affinity; POMs are more prone to bind with $3CL^{pro}$ than with some organic compounds; for the POMs/$3CL^{pro}$complex, the OTi_2 in POMs is the vital element for electrostatic interaction, and the electrostatic binding energy is strong enough to keep the complex stable.

Keywords: SARS; $3CL^{pro}$; Molecular dynamics; Docking; Polyoxometalates (POMs)

1. Introduction

Severe acute respiratory syndrome (SARS), a suddenly happened worldwide pandemic in 2003, was suffered by thousands of people and killed hundreds of them. Coronavirus was identified as the etiologic agent of SARS [1,2]. SARS coronavirus (SARS-CoV) is a positive strand RNA virus. The plasmid of SARS-CoV includes six kinds of proteins: nucleocapsid (N), spike (S), membranes (M), small envelope (E), polymerase and 3c like (3CL) hydrolytic protease. There are 18 complete genome sequences from different resources that have been determined. Sequence analysis show these genomes are different but not too much, especially its main protease, the 3CL protease($3CL^{pro}$) is relatively conserved in the SARS genome and thus can be taken as one of the key targets for anti-SARS drug design [1–5].

The $3CL^{pro}$ is the key protein during virus replication; its main function is to hydrolyze the polymerase expressed by the virus. In SARS-CoV the nonstructural gene (namely the enzyme copy gene) code for two overlapped polypeptides: pp1a (486 kDa) and ORF1b (790 kDa). They conduct almost all functions needed during the course of virus replication as well as transcription. Polypeptides with different functions are mostly produced from these two polypeptides and this kind of crack procedure is just mainly dependent on the $3CL^{pro}$ [3,4]. The catalytically active site of SARS-CoV $3CL^{pro}$ has been shown to be Cys145/His41 [2,6,7], which is conserved in this protein. Therefore, designing drugs for this $3CL^{pro}$ should inhibit SARS infection effectively.

Polyoxometalates (POMs) are oxygen rich class of inorganic cluster systems exhibiting remarkable chemical and physical properties, which have been applied to various

* Corresponding author. Tel.: +86 4315099108; fax: +86 43156840009.
E-mail address: zmsu@nenu.edu.cn (Z. Su).

0162-0134/$ - see front matter © 2006 Elsevier Inc. All rights reserved.
doi:10.1016/j.jinorgbio.2006.08.013

fields such as catalysis, materials and medicines [8–10]. POMs perform significant biological activities, with high efficacy and low toxicity. In particular, the sizes and globular structural motifs of many POMs are similar, and in some cases nearly identical to some water-soluble fullerene derivatives showing fairly good anti-HIV-1P activity [11]. Liu and her co-workers have investigated POMs compounds such as PW, SiW, PMo, and SiMo. Their results show that some POMs possess lower cell virulence and higher anti-HIV activity [8,12–18].

Among various POMs, the di-Ti-substituted α-Keggin type structure $[\alpha\text{-}PTi_2W_{10}O_{40}]^{7-}$ isomers are of particular interest because of their high catalytic activity and capability of inhibiting replication of several types of DNA or RNA viruses. Many papers report that Ti-containing α-Keggin POMs show obvious inhibition activity to HIV-1 [19–27]. It is very significant to explore the inhibition potency of α-Keggin POMs to SARS-CoV. Firstly, whether POMs interact with the SARS main functional protease of $3CL^{pro}$; secondly, what the interaction mechanism should be; and above all, it is of great significance to explore molecular mechanism and molecular dynamics mechanism when studying problems related to POMs. In this investigation, the α-Keggin type POM isomers including $[\alpha\text{-}1,5\text{-}PTi_2W_{10}O_{40}]^{7-}$, $[\alpha\text{-}1,6\text{-}PTi_2W_{10}O_{40}]^{7-}$, $[\alpha\text{-}1,11\text{-}PTi_2W_{10}O_{40}]^{7-}$, $[\alpha\text{-}1,4\text{-}PTi_2W_{10}O_{40}]^{7-}$, $[\alpha\text{-}1,2\text{-}PTi_2W_{10}O_{40}]^{7-}$ were selected as candidates for SARS-CoV $3CL^{pro}$ inhibitors. Binding energy was compared, hydrogen bonds formation and electrostatic interaction were analyzed, active site key residues were identified and the interaction mechanism was also discussed at molecular level.

2. Models and methods

2.1. Equilibrated conformation of $3CL^{pro}$

The three dimensional crystal structures and the active site information of SARS-CoV $3CL^{pro}$ were obtained by experimental methods recently [2,6]. SARS-CoV $3CL^{pro}$ consists of two promoters nearly perpendicular with each other, and each one of them has three structure domains. Domains I, II are of anti-parallel sheets, while domain O forms an anti-parallel global conformation including five α-helixes.

The crystal structure coordinate of $3CL^{pro}$ was downloaded from the protein Database (PDB ID: 1UK4, Resolution = 2.5 Å). The $3CL^{pro}$ is made up of two protomers: protomer A and protomer B, each one of them consists of 306 amino acids [28]. Biopolymer/Insight II module was used to repair the lost coordinates. The side residues were optimized and modified properly to decrease geometry collision with surrounding atoms. Molecular mechanics calculation was performed after molecular dynamics [29–32]. After the energy converged, the conformation with the lowest energy was taken as the $3CL^{pro}$ analysis structure. The final equilibrated conformation in solution of SARS $3CL^{pro}$ is shown in Fig. 1.

The SARS-CoV $3CL^{pro}$ model is evaluated with the Profile-3D/Insight II module [33], and the evaluation result is shown in Fig. 2. It is clearly shown that most residues are modeled reasonably, which indicates the structure is modeled successfully. Four residues of Arg-A60, Ser-A62, His-A64 and Lys-A236 are poorly built; the reason should be that these hydrophobic residues are not well shielded from solvent in the model. Fortunately, all the four residues locate far away from the enzyme active site, so they should have little influence on subsequent investigations.

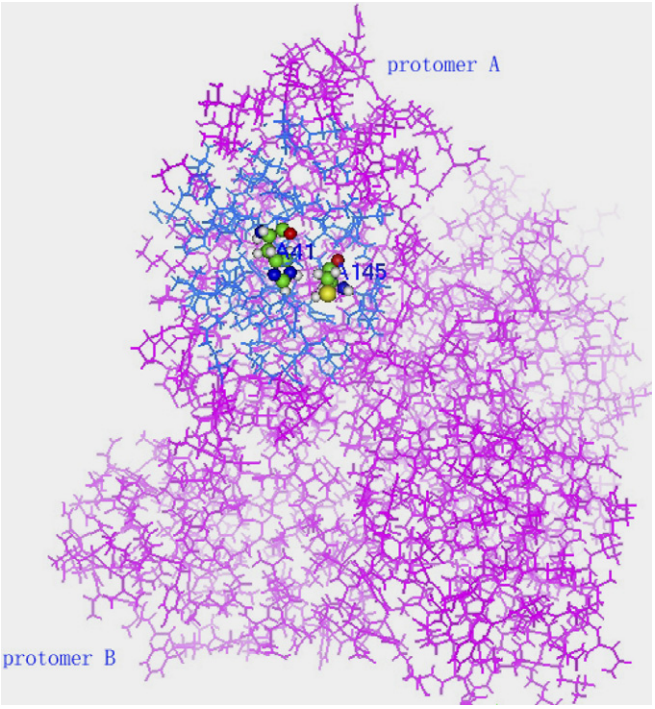

Fig. 1. The equilibrated conformation in solution of SARS $3CL^{pro}$ dimer. The catalytic residues of Cys145 and His41 are represented in ball-and-stick.

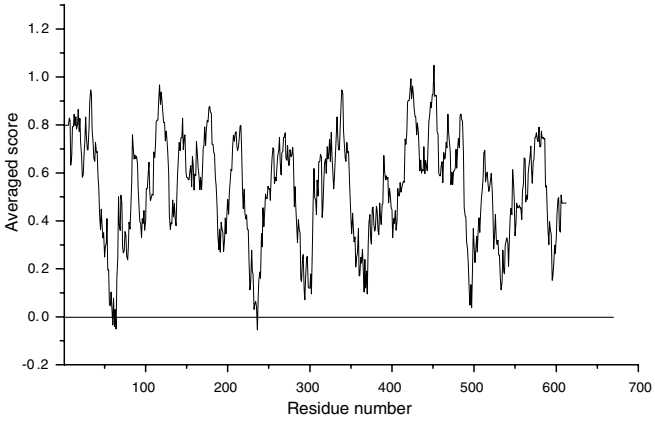

Fig. 2. Profile-3D evaluation of the SARS-CoV $3CL^{pro}$ model.

2.2. Selecting the POMs compounds

Recently, we have systematically investigated the electronic properties, redox properties, protonation, and stability of five POM $[\alpha\text{-PTi}_2\text{W}_{10}\text{O}_{40}]^{7-}$ isomers. Our results revealed that the bridging oxygens (OTi_2 and OTiW) as well as the terminal oxygens (OTi), act as nucleophilic centers. In particular, the bridging oxygens bond to two titaniums (OTi_2) in $[\alpha\text{-1,4-PTi}_2\text{W}_{10}\text{O}_{40}]^{7-}$ and $[\alpha\text{-1,2-PTi}_2\text{W}_{10}\text{O}_{40}]^{7-}$exhibit strong nucleophilic activity [26]. The three dimensional structural models of the five $[\alpha\text{-PTi}_2\text{W}_{10}\text{O}_{40}]^{7-}$ isomers are shown in Fig. 3. A short-hand notation is used for these isomers, without oxygen atoms, tungsten atoms and anion charge. (e.g., $[\alpha\text{-1,5-PTi}_2\text{W}_{10}\text{O}_{40}]^{7-} = \text{1,5-PTi}_2$, $[\alpha\text{-1,6-PTi}_2\text{W}_{10}\text{O}_{40}]^{7-} = \text{1,6-PTi}_2$, $[\alpha\text{-1,11-PTi}_2\text{W}_{10}\text{O}_{40}]^{7-} = \text{1,11-PTi}_2$, $[\alpha\text{-1,4-PTi}_2\text{W}_{10}\text{O}_{40}]^{7-} = \text{1,4-PTi}_2$ and $[\alpha\text{-1,2-PTi}_2\text{W}_{10}\text{O}_{40}]^{7-} = \text{1,2-PTi}_2$).

2.3. Docking study of POMs with SARS-CoV 3CL^{pro}

Charge properties of POMs were obtained from quantum chemical calculation employing the density-functional theory (DFT) method. The parameters for atomic point charges were not available for heavy metal atoms of the tungsten atom and titanium atom in POMs, this may affect the precise computation value of charge distribution and absolute values of binding energy. However, the general interaction position of POMs with 3CL^{pro} should not change because it was based on energy difference instead of the absolute values. An assumption made in this study was that neither the enzyme nor the inhibitors undergo major structural changes on binding. The five POMs of 1,5-PTi_2, 1,6-PTi_2, 1,11-PTi_2, 1,4-PTi_2, and 1,2-PTi_2 were docked respectively in the active site of SARS 3CL^{pro}. More than ten slightly different docking positions were examined across the Affinity/Insight II [34]. The enzyme–inhibitor complex with the lowest energy was chosen for further examination.

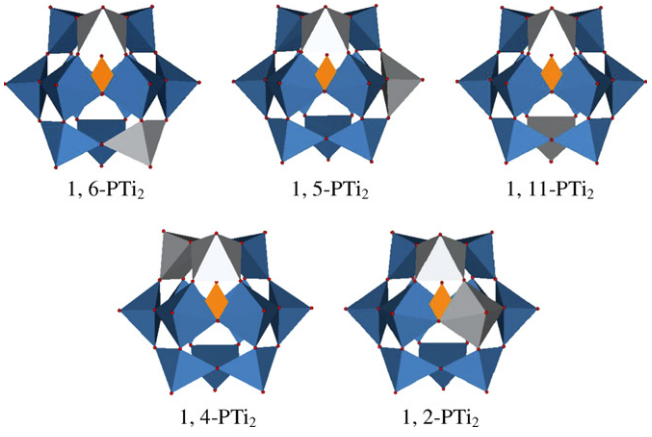

Fig. 3. The three-dimensional structural models of the five $[\alpha\text{-PTi}_2\text{W}_{10}\text{O}_{40}]^{7-}$ POMs.

3. Results and discussion

Docking simulations of the five POM isomers of 1,6-PTi_2, 1,5-PTi_2, 1,11-PTi_2, 1,4-PTi_2, 1,2-PTi_2 with SARS 3CL^{pro} were carried out using Affinity/Insight II, the results are shown in Fig. 4 and Table 1.

The representative structure of POM/3CL^{pro} complexes is shown in Fig. 4. The results show that all the five POM ligands interact with the 3CL^{pro} receptor just in the active site region including the catalytic residues. Hydrogen bonds are formed between POMs and several key residues including the catalyst residues of 3CL^{pro} His41/Cys145. The ligand–receptor interaction of POMs/3CL^{pro} generally causes energy decreasing and conformation changing; accordingly these changes should influence the enzyme catalytic activity of the SARS-CoV 3CL^{pro}.

Binding energy of the five Ti-containing α-Keggin POMs of 1,5-PTi_2, 1,6-PTi_2, 1,11-PTi_2, 1,4-PTi_2 and 1,2-PTi_2 with the SARS-CoV 3CL^{pro} receptor are summarized in Table 1. Where "Δ" represents energy difference originated from steric hindrance between POMs and 3CL^{pro}, "Δ_1" represents electrostatic energy changing of the complex, and "Δ_2" is the total energy changing. As is shown in the results that, for all these five ligand–receptor complexes, the electrostatic energy (Δ_1) both decrease remarkably, which indicates that the highly negative charged POM inhibitors interact with the 3CL^{pro} and therefore cause electrostatic energy to decrease. Furthermore, the electrostatic interaction is strong enough to overcome the

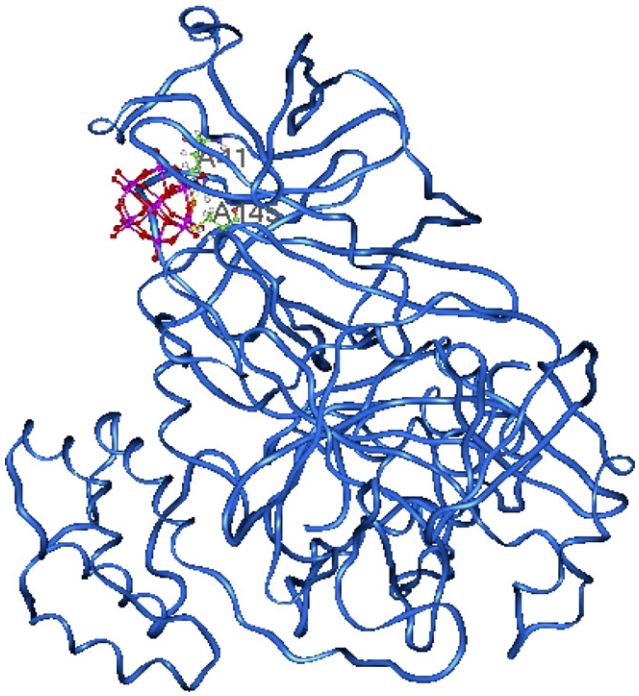

Fig. 4. The representative structure of POM/SARS-CoV 3CL^{pro} complex. The 3CL^{pro} is represented in cartoon, while binding site and POM are represented in ball-and-stick.

Table 1
Binding energy between ligand and receptor (KJ/mol)

	E^{Pot}	Δ	E^{Nonb}	Δ_1	$\Delta_2(\Delta+\Delta_1)$
$3CL^{pro}$	−9728.458		−13646.040		
1,2-$PTi_2/3CL^{pro}$	−9690.838	37.620	−13755.647	−109.607	−71.987
1,4-$PTi_2/3CL^{pro}$	−9689.251	39.207	−13753.616	−107.576	−68.369
1,11-$PTi_2/3CL^{pro}$	−9688.869	39.589	−13748.752	−102.712	−63.123
1,5-$PTi_2/3CL^{pro}$	−9691.295	37.163	−13749.754	−103.714	−66.551
1,6-$PTi_2/3CL^{pro}$	−9691.009	37.449	−13749.227	−103.187	−65.738

Note: Δ is the energy change originating from the steric hindrance.
Δ_1 is the energy change of electrostatic energy.
Δ_2 is the total energy change of electrostatic energy plus steric hindrance.

unfavorable steric effects, therefore results in total negative energy (Δ_2) in all the five complexes. Binding energy is an important criterion for reliable virtual screening. Several researches have performed virtual screening study of SARS-CoV $3CL^{pro}$ using small molecular like AG7088 as reference molecule [35,36]. As is shown in our investigation that, binding energy of POM/$3CL^{pro}$ complex is much higher than that of some small organic molecules. This indicates that POMs may even more prone to bind with $3CL^{pro}$ than small organic molecules. What is more, an important conclusion can be drawn from our study is that, the total binding energies of the five complex systems follow the order of 1,2-$PTi_2/3CL^{pro}$ > 1,4-$PTi_2/3CL^{pro}$ > 1,5-$PTi_2/3CL^{pro}$ > 1,6-$PTi_2/3CL^{pro}$ > 1,11-$PTi_2/3CL^{pro}$, which can provide perfectly well interpretation on the relative stability of the five POM/$3CL^{pro}$ complexes.

Relative information about hydrogen bonds interaction is listed in Table 2. There are eight hydrogen bonds formed in the 1,6-$PTi_2/3CL^{pro}$ complex, and six hydrogen bonds in the 1,2-$PTi_2/3CL^{pro}$ complex. Moreover, it is clearly shown that the $OTi_2$of POMs contributes much to hydrogen bond formation within all the five ligand-receptor complexes. Our former DFT calculation have shown that in these POM isomers, the charge loading of OTi_2 is much stronger than that of other bridging oxygen and terminal oxygen. That should be the reason why the two systems of the 1,2-$PTi_2/3CL^{pro}$ complexes and the 1,4-$PTi_2/3CL^{pro}$ complex are much more stable than the others. It should be noticed that there are only six hydrogen bonds in 1,11-$PTi_2/3CL^{pro}$ and the terminal oxygen also attends hydrogen bonds formation. Our quantum chemistry calculation also proved that the charge loading of the terminal oxygen is smaller than that of OW_2. Therefore, it is easy to interpret why the complex of 1,11-$PTi_2/3CL^{pro}$ is the least stable one among all the five ligand–receptor complex systems.

In addition, it should be noticed from the hydrogen bonding interaction shown in Fig. 5 that, POMs interact with $3CL^{pro}$ in the active site region with several positive charged amino residues including the active site catalysis residues. Those key residues for ligand–receptor interaction including Thr26, His41, Cys44, Asn142, Cys145, Clu166, Asp187 and Gln189, are all polarity residues, this make them easy to form hydrogen bonds meshwork and increase the complex stability. What is more, during the course of POMs/SARS-CoV $3CL^{pro}$ complex formation, the atom charge loading properties and the electrostatic characteristic are very vital elements that keep the enzyme–inhibitor interaction. Therefore, the atom charge loading property and the electrostatic characteristic are two vital elements keeping POM/$3CL^{pro}$ complex stable and deserve paying

Table 2
Binding site and H-bond formation (H-bond length: Å)

Complex	$3CL^{pro}$ residue	Ligand atom	Distance
1,2-$PTi_2/3CL^{pro}$	A46:O	O11	2.29
	A145:O	O16	2.75
	A164:O	O22	1.75
	A41:ND1	O22	2.87
	A41:ND1	O23	1.40
	A41:ND1	O25	2.56
	A189:OE1	O28	0.76
	A26:O	O41	1.96
1,4-$PTi_2/3CL^{pro}$	A166:O	O6	2.04
	A41:HE2	O20	2.11
	A166:OE2	O44	2.98
	A41:ND1	O47	2.35
	A143:O	O50	1.84
	A145:HN	O50	2.47
1,11-$PTi_2/3CL^{pro}$	A25:OG1	O12	1.47
	A41:O	O12	2.96
	A26:O	O19	2.51
	A187:O	O22	2.92
	A166:O	O27	2.86
	A142:OD1	O42	2.51
1,5-$PTi_2/3CL^{pro}$	A119:OD1	O9	2.37
	A145:HN	O9	2.13
	A166:OE1	O19	1.39
	A26:O	O22	1.44
	A46:O	O29	1.69
	A41:O	O36	1.48
	A164:O	O39	1.92
	A166:O	O42	2.76
	A41:HE2	O43	2.07
1,6-$PTi_2/3CL^{pro}$	A25:O	O45	2.28
	A26:O	O52	2.13
	A26:HN	O39	0.67
	A41:O	O50	2.53
	A41:ND1	O42	2.65
	A41:HE2	O33	1.96
	A44:O	O47	2.93
	A142:O	O48	2.84

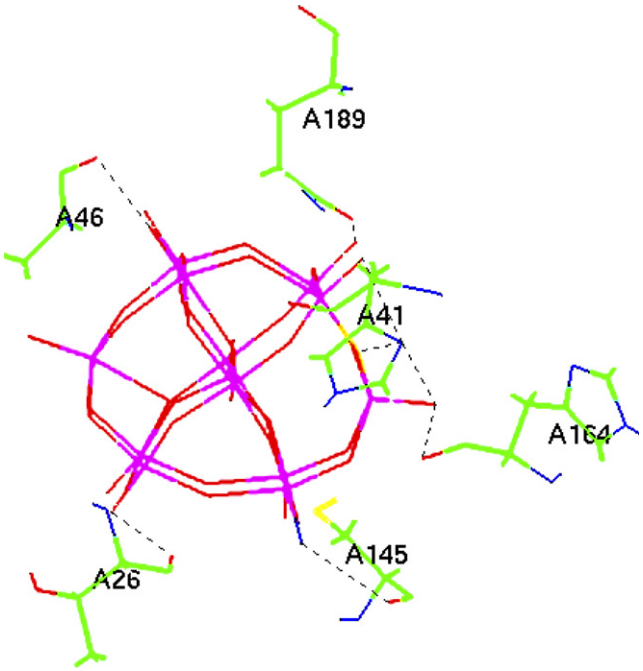

Fig. 5. Key residues and hydrogen bond interactions of POM/3CL^{pro} complex.

much more attention when consider POMs/enzyme interactions. POMs interact with 3CL^{pro} in the active site region with obvious electrostatic property compensation adjustment, accordingly it may preclude the hydrolysis of the two polypeptides expressed by SARS virus, and therefore may cut off the approach of virus replication. The kinetics and binding studies, conducted after molecular modeling, are both in remarkable agreement with relative results.

4. Conclusions

Docking investigations on five POM ($[\alpha\text{-}PTi_2W_{10}O_{40}]^{7-}$) isomers with SARS-CoV 3CL^{pro} were performed using computer assisted molecular simulation technology. The investigation results show that: (1) POMs interact with the 3CL^{pro} receptor in enzyme active site region, with several polarized residues including the enzyme catalyst residues of His41/Cys145; (2) The total binding energies of the five POM/SARS-CoV 3CL^{pro} complexes lead to the following order of complex stability: 1,2-PTi_2/3CL^{pro} > 1,4-PTi_2/3CL^{pro} > 1,5-PTi_2/3CL^{pro} > 1,6-PTi_2/3CL^{pro} > 1,11-PTi_2/3CL^{pro}. (3) Electrostatic energy and hydrogen bond interaction contribute much to the enzyme–inhibitor complex formation between POMs and SARS-CoV 3CL^{pro}. The atom charge loading property and electrostatic characteristic are very vital elements that keep the enzyme–inhibitor interaction. In POMs, the electronegative OTi_2 oxygen contributes much for electrostatic energy interactions. As a result, those POMs with OTi_2 oxygen should form relative stable complex with protein receptors. The simulation results provide important information for POMs/SARS-CoV 3CL^{pro} interaction, and may provide insights for anti-SARS drug design.

5. Abbreviations

POMs	Polyoxometalates
HIV	human immunodeficiency virus
SARS-CoV	SARS coronavirus
SARS 3CL^{pro}	SARS 3c like protease
DFT	density-functional theory
1,5-PTi_2	$[\alpha\text{-}1,5\text{-}PTi_2W_{10}O_{40}]^{7-}$
1,6-PTi_2	$[\alpha\text{-}1,6\text{-}PTi_2W_{10}O_{40}]^{7-}$
1,11-PTi_2	$[\alpha\text{-}1,11\text{-}PTi_2W_{10}O_{40}]^{7-}$
1,4PTi_2	$[\alpha\text{-}1,4\text{-}PTi_2W_{10}O_{40}]^{7-}$
1,2-PTi_2	$[\alpha\text{-}1,2\text{-}PTi_2W_{10}O_{40}]^{7-}$

Acknowledgements

We gratefully acknowledge the financial support from the National Natural Science Foundation of China (Projects 20373009 and 20573016) and Youth Fund of Northeast Normal University (No. 111494017, 20060305). All the work including molecular modeling, molecular dynamics and molecular docking are carried out on SGI GRAPHICS work station in State Key Laboratory of Theoretical and Computational Chemistry of Jilin University, using Insight II molecular simulating software package of MSI, with modules including Biopolymer, Homology, Discover3, Docking/Affinity, and Delphi [37].

Appendix A. Supplementary data

Supplementary data associated with this article can be found, in the online version, at doi:10.1016/j.jinorgbio.2006.08.013.

References

[1] P.A. Rota, M.S. Oberste, S.S. Monroe, Science 300 (2003) 1394–1399.
[2] K. Anand, J. Ziebuhr, P. Wadhwani, Science 300 (2003) 1763–1767.
[3] H.L. Liu, J.C. Lin, H. Yih, Chem. Phys. Lett 401 (2005) 24–29.
[4] J.S.M. Peiris, S.T. Lai, L.L.M. Poon, Lancet 361 (2004) 1319–1325.
[5] Y.C. Lan, H.F. Liu, Y.P. Shih, Infect. Gene. Evol. 5 (2005) 261–269.
[6] K. Anand, G.J. Palm, J.R. Mesters, EMBO. J. 21 (2002) 3213–3224.
[7] L.L.M. Poon, C.S.W. Leung, M. Tashiro, Clin. Chem. 50 (2004) 1050–1052.
[8] M.L. Xiang, S.X. Xiao, Z.R. Yuan, Res. Appl. 2 (2000) 621–625.
[9] D.C. Erik, Rev. Med. Virol. 10 (2000) 255–257.
[10] D.C. Erik, Med. Res. Rev. 22 (2002) 531–565.
[11] D.A. Judd, J.H. Nettles, N. Nevins, J. Am. Chem. Soc. 123 (2001) 886–897.
[12] S.X. Liu, L. Wang, E.B. Wang, J. Chin. Rare. Earth. Soc. 15 (1997) 59–63.
[13] C.N. Chen, C.P.C. Lin, K.K. Huang, Altern. Med. 2 (2005) 209–215.
[14] M.L. Xiang, Z.G. Zhao, Z.R. Yuan, J. Biomed. Eng. 2 (2002) 291–297.
[15] Y. He, H. Lu, P. Siddiqui, J. Immunol. 174 (2005) 4908–4915.
[16] S.X. Liu, Y.G. Li, Z.B. Han, Chem. J. Chin. Univ. 23 (2002) 778–782.
[17] H.J. Zhai, S.X. Liu, Y.X. Li, Chin. J. Inorg. Chem. 21 (2005) 1798–1802.

[18] S.X. Liu, C.L. Wang, M. Yu, Acta. Chin. Sinica. 63 (2005) 1069–1074.
[19] Y. Take, Y. Tokutake, Y. Inouye, Antiv. Res. 15 (1991) 113–124.
[20] Y. Inouye, Y. Fujimoto, M. Sugiyama, Bio. Pharm. Bull. 18 (1995) 996–1000.
[21] Y. Inouye, Y. Tokutake, J. Kunihara, Chem. Pharm. Bull. 40 (1992) 805–807.
[22] J.T. Rhule, C.L. Hill, D.A. Judd, Chem. Rev. 98 (1998) 327–357.
[23] M. Witvrouw, H. Weigold, C. Pannecouque, J. Med. Chem. 43 (2000) 778–783.
[24] S. Shigeta, S. Mori, E. Kodama, Antiv. Res. 58 (2003) 265–271.
[25] J. Liu, E.B. Wang, L.N. Ji, Prog. Chem. 18 (2006) 114–119.
[26] W. Guan, L.K. Yan, Z. M. Su. Inorg. Chem. 44 (2005) 100–109 (the nomenclature is incorrect).
[27] C. Shao, D.H. Hu, Z.M. Su, Chem. J. Chin. Univ. 26 (2005) 1512–1516.
[28] H.T. Yang, M.J. Yang, Y. Ding, Proc. Natl. Acad. Sci. USA 100 (2003) 13190–13195.
[29] C.Z. Guo, Z.Y. Xuan, R.S. Chen, Chin. J. Biochem. Mol. Biol. 18 (2002) 499–505.
[30] S. Barlow, A.L. Rohl, S. Shi, J. Am. Chem. Soc. 188 (1996) 7578–7592.
[31] R. Luthy, J.U. Bowie, D. Eisenberg, Nature 356 (1992) 83–85.
[32] J. Peiris, S. Lai, L. Poon, Lancet 361 (2003) 1319–1325.
[33] Discover 3 User Guide, San Diego, MSI, USA, 1999.
[34] P.A. Greenidge, B. Carlsson, L.G. Bland, J. Med. Chem. 41 (1998) 2503–2512.
[35] L. Chen, C. Gui, X. Luo, J. Virol. 79 (2005) 7095–7103.
[36] C.W. Lin, C.H. Tsai, F.J. Tsai, FEBS Lett. 574 (2004) 131–137.
[37] Insight II, Version 98.0, San Diego, MSI, 1998.